Current Cardiology Reports (2019) 21: 103
https://doi.org/10.1007/s11886-019-1196-7

CARDIO-ONCOLOGY (SA FRANCIS AND RB MORGAN, SECTION EDITORS)

The Assessment of Cardiac Masses by Cardiac CT and CMR Including Pre-op 3D Reconstruction and Planning

Stephen Liddy[1] · Colin McQuade[1] · Kevin P. Walsh[2] · Bryan Loo[3] · Orla Buckley[1]

Published online: 31 July 2019

Abstract

Purpose of Review The purpose of this review is to (1) review the recent evidence examining the use of CT and CMR in the assessment of a suspected cardiac mass, (2) summarize the typical imaging features of the most common cardiac masses, and (3) examine the latest developments in the use of three-dimensional reconstructions and models in the preoperative assessment of a cardiac mass.

Recent Findings CMR can distinguish between tumors and non-tumor masses and between benign and malignant mass with a high degree of accuracy.

Summary CT and CMR are complementary tools in the evaluation of cardiac masses. CMR is the preferred initial imaging modality due to its versatile imaging planes and superior tissue characterization. CT better depicts calcification and has a higher spatial resolution compared with CMR, which is of particular importance in preoperative planning. CT also offers a valuable alternative in those with contraindications to CMR. Three-dimensional reconstructions, particularly of CT datasets, are a valuable adjunct in the preoperative assessment of a cardiac mass and may allow a better appreciation of the margins of the mass and its relationship with surrounding structures. Three-dimensional printing is an emerging technology which may be of additional value in selected patients with a cardiac mass.

Keywords Heart neoplasm · Computed tomography · Magnetic resonance imaging · Imaging · Three-dimensional

This article is part of the Topical Collection on *Cardio-Oncology*

✉ Stephen Liddy
stephenliddy@gmail.com

Colin McQuade
colin.mcquade@tuh.ie

Kevin P. Walsh
kpjwalsh@icloud.com

Bryan Loo
bryan.loo@tuh.ie

Orla Buckley
orla.buckley@tuh.ie

[1] Department of Radiology, Tallaght University Hospital, Tallaght, Dublin 24, Ireland

[2] Department of Cardiology, Mater Misericordiae University Hospital, Dublin 1, Ireland

[3] Department of Cardiology, Tallaght University Hospital, Tallaght, Dublin 24, Ireland

Introduction

With the widespread and routine use of echocardiography and computed tomography (CT), the incidental detection of a cardiac mass is not uncommon. Cardiac masses can be categorized as non-neoplastic or neoplastic. Non-neoplastic masses, or pseudotumors, are the most common cardiac masses, with thrombi, pericardial cysts, and prominent anatomical structures frequently mimicking true cardiac neoplasms.

True neoplasms can be subdivided into primary or secondary tumors. Primary cardiac tumors are exceptionally rare with autopsy studies estimating an overall prevalence of 0.0002–0.3% [1, 2]. Of these, approximately 75% are benign. Myxomas represent half of all benign primary cardiac tumors, followed by papillary fibroelastomas, lipomas, and hemangiomas [3, 4]. The remaining 25% of primary cardiac masses are malignant, of which the vast majority are sarcomas. Angiosarcomas and undifferentiated sarcomas are the most common histological subtype of malignant cardiac mass in adults, whereas rhabdomyosarcomas are the most commonly encountered subtype in children [5].

Secondary cardiac tumors (metastases) are 30–40 times more common than primary tumors and can spread to the heart by hematogenous dissemination, lymphatic spread, venous extension, or direct invasion [6]. Melanoma and thoracic neoplasms such as lung, breast, and esophageal carcinomas are the most frequently implicated primaries.

It has become mandatory for radiologists and cardiologists reporting cardiac imaging to be familiar with the imaging appearance of the most common cardiac masses. In this article, we review the recent evidence examining the use of CT and cardiac magnetic resonance imaging (CMR) in the assessment of a suspected cardiac mass and summarize the typical imaging features of the most common cardiac masses. We also examine the latest developments in the use of three-dimensional (3D) reconstructions and models in the preoperative assessment of a cardiac mass.

Advantages and Disadvantages of Cardiac CT and CMR

CMR is the preferred imaging modality in the workup of a cardiac mass due to its excellent soft tissue characterization, high temporal resolution, and multiplanar imaging capabilities—a key advantage given the complex anatomy of the heart. A lack of ionizing radiation is a further advantage and is of particular relevance in the pediatric population. CMR however has several limitations. Considerable patient cooperation is required to achieve high-quality images, which may prove difficult in claustrophobic patients or in those unable to perform the required breath-holds. High-quality imaging is reliant on electrocardiographic (ECG)-gating and may suffer from image degradation in those with arrhythmias. MR-compatible and MR-safe implantable cardiac devices are becoming more widespread; however, there are many patients with non-MR-compatible devices [7]. Furthermore, not all centers have the necessary expertise or precautions in place to safely image those with compatible devices. CMR is also susceptible to artifact from implantable cardiac devices which can significantly degrade image quality.

Cardiac CT is commonly employed as a complementary imaging modality [8]. Technological advances such as submillimeter detector arrays enabling submillimeter spatial resolution, accelerated gantry rotation times allowing improved temporal resolution, and ECG-gating to reduce artifact from cardiac motion have resulted in improved imaging quality [9, 10]. The superior spatial resolution of CT compared with CMR allows for accurate assessment of the location of the mass, the degree of local invasion, as well as encasement of the coronary arteries or involvement of any adjacent valvular apparatus. Additionally, calcification and macroscopic fat are readily detected. For example, heterotopic calcification in the region of the mitral valve can have a mass-like appearance on CMR but is easily identified on CT. The primary disadvantages of CT include exposure to ionizing radiation, a small risk of contrast-related adverse events, and limited tissue characterization and temporal resolution relative CMR. However, prospective ECG-gating has reduced radiation exposure, which is now in the 1–2 mSv range for CT coronary angiography performed with contemporary equipment [11, 12].

In practice, TTE and CMR are the preferred primary imaging modalities in the diagnosis, assessment, and monitoring of a cardiac mass. CT offers a valuable complementary tool due to its superior spatial resolution and ability to detect calcification.

Benign vs Malignant Masses

Accurately distinguishing between benign and malignant tumors is important for patient management and surgical planning. As malignant tumors have a high risk of local recurrence, standard resection techniques are often inadequate and a more aggressive approach is warranted. Neoadjuvant chemotherapy, radical surgical resection, and autotransplantation may be considered in such cases. As not all lesions are amenable to biopsy, preoperative imaging plays an important role in differentiating between benign and malignant tumors. Table 1 summarizes the most common benign and malignant masses by their typical location.

No recent studies have evaluated the accuracy CT in distinguishing between benign and malignant masses; however, several have examined the diagnostic performance of CMR. Kassi et al. prospectively compared the imaging features on CMR of 27 benign tumors and 39 malignant tumors and found a significant difference between the two groups [13•]. Malignant tumors were more likely to have irregular borders (80% vs 26%) and were more likely to infiltrate into the free wall (54% vs 0%) or adjacent structures (49% vs 0%). Large tumor size (> 5 cm) and concurrent pericardial effusion were also associated with malignancy. Likewise, enhancement on first pass perfusion was evident in all malignant tumors but only one third of benign tumors. Late gadolinium enhancement was also present in all malignant tumors but was also seen in 60% of benign tumors. Overall, no single feature could be used to definitively distinguish between benign and malignant tumors; however, tumor size, local invasion and enhancement on first pass perfusion were the strongest predictors of malignancy.

A 2012 series of 161 patients, of whom 42 subsequently had a cardiac mass proven at biopsy, found CMR was 89% sensitive and 100% specific at distinguishing between benign and malignant masses and was 94% sensitive and 91% specific at distinguishing between tumor and non-tumor masses [14]. In a 2016 review examining the value CMR in the assessment of a suspected mass on CT or transthoracic

Table 1 Benign and malignant masses by location, with characteristic imaging features

	Benign	Malignant
Any chamber	Lipoma (fat density/signal)	Metastasis
	Hemangioma (avid enhancement)	Rhabdomyosarcoma (intramural)
Right atrium		Angiosarcoma (polypoid or infiltrative)
		Lymphoma
Right ventricle	Fibroma (solitary, LGE enhancement)	Angiosarcoma (polypoid or infiltrative)
	Rhabdomyoma (multiple)	Lymphoma
Left atrium	Myxoma (stalk-like attachment)	Sarcoma, other than angiosarcoma
	Thrombus (variable signal, no enhancement*)	
Left ventricle	Fibroma (solitary, LGE enhancement)	
	Rhabdomyoma (multiple)	
	Thrombus (variable signal, no enhancement*)	
Valvular	Papillary fibroelastoma	
	Vegetation	
	Thrombus (variable signal, no enhancement*)	

*Chronic thrombus may occasionally show mild peripheral enhancement due to fibrosis

echocardiography (TTE), CMR correctly identified malignant masses in 19/19 (100%) cases and correctly characterized thrombus vs benign masses in 59/66 (89%) cases [15].

A 2016 study comparing CMR and TTE in 50 patients reported that CMR identified 6 masses missed on TTE (4 of which were outside the heart) and was more accurate than TTE at predicting the histopathologic diagnoses (77% vs 43%) [16]. And lastly, a 2018 series of 158 patients who underwent CMR for a suspected cardiac mass on TTE, CMR confirmed the presence of a mass in 72% of cases (114/158). In 15.8% (18/114), CMR and TTE were in agreement regarding the presence and classification of the mass. Whereas in 53.5% (61/114), CMR and TTE agreed as to the presence of a mass, but not as to the specific classification. However, as histopathology results were not available, the sensitivity and specificity of each modality could not be determined [17].

In summary, CMR distinguishes between benign and malignant masses (also between tumor and non-tumor masses) with a high degree of accuracy, with tumor size, local invasion, and enhancement on first pass perfusion serving as the most reliable predictors of malignancy.

Benign Masses

Myxoma

Myxomas are the most common primary cardiac tumor and typically occur in the 4th–7th decade, with a mean age of presentation of 53 years [3, 18]. A majority of cases occur in the left atrium and are solitary, although they may originate in any chamber, inferior vena cava or from the valve leaflets [18]. Most occur sporadically but 10% are associated with several familiar syndromes including Carney complex (cardiac and mucocutaneous myxomas, pigmented skin lesions schwannomas, and endocrine tumors), LAMB syndrome (lentigines, atrial myxomas, blue nevi), and NAME syndrome (nevi, atrial myxoma, myxoid neurofibroma, ephelides) [19, 20]. In cases where there is a syndromic association, atypical intra cardiac locations and multiplicity may be seen.

The typical appearance is of a polypoid intracavitary mass within the left atrium, attached to the fossa ovalis by a stalk. On non-contrast-enhanced CT, myxomas appear as smooth, lobulated, hypodense masses. Calcification may be present but is more commonly seen when located in the right atrium. On contrast-enhanced CT, myxomas appear as intracavitary filling defects. Necrosis or hemorrhage may give rise to a heterogenous enhancement pattern following the administration of contrast. Myxomas may be detected incidentally at CT and can often diagnosed with confidence without the need for CMR due to their typical appearance. The high spatial resolution of CT enables precise location of the size and insertion of the stalk.

On CMR, myxomas appear isointense to myocardium on T1-weighted images and hyperintense on T2-weighted images due to a high extracellular water content. As on CT, contrast enhancement is typically heterogenous. Cine images are particularly useful as myxomas are often highly mobile, especially when pedunculated, and may prolapse across the mitral valve leading to obstructive symptoms [21].

Surgical resection is the treatment of choice. Recurrence rates range from 4 to 7% in isolated myxomas and from 10 to 21% in those with Carney complex, necessitating close follow-up in such patients. [22]

Lipoma

Lipomas are the second most common primary cardiac neoplasms accounting for 10% of cases. They are well-circumscribed, encapsulated masses of neoplastic adipose cells [3]. They most commonly arise from the epicardial surface but may also originate from the mid-myocardial or subendocardial layers [23]. They are often discovered incidentally and patients typically remain asymptomatic. If large, lipomas may rarely lead to arrhythmias or obstructive symptoms.

On CT, lipomas appear as homogenous, fat-attenuation mass (Hounsfield units less than − 50). On CMR, they appear hyperintense on T1-weighted sequences and suppress completely when fat suppression is applied. Thin septations may be visible on CMR or on thin slice CT. As lipomas are avascular, they do not enhance post-contrast. Both CT and CMR can reliably diagnose cardiac lipomas but CT often suffices.

Lipomatous hypertrophy of the interatrial septum (LHIAS) is not a true neoplasm and is but can be reliably distinguished from a lipoma on CT and CMR by its characteristic appearance. LHIAS is not encapsulated and spares the fossa ovalis producing a bilobed or dumbbell configuration [24]. LHIAS can contain metabolically active brown fat and therefore can present as an incidental pseudotumor on PET/CT [25]. Occasionally, it can also have a mass-like appearance on TTE.

Papillary Fibroelastoma

Papillary fibroelastomas are the third most common primary cardiac neoplasm accounting for approximately 10% of cases [26]. The mean age of presentation is 60 years and men and women are affected equally [27]. Often presenting incidentally, their prevalence in the general population is uncertain; however, one autopsy series reported an overall prevalence of 0.33% [28].

Papillary fibroelastomas have a frond-like morphology and consist of dense connective tissue lined by endothelium. They usually originate from the cardiac valves but can also arise from the atrial or ventricular wall [27, 29]. Given the high spatial resolution of CT, these lesions are being increasingly detected incidentally. Papillary fibroelastomas are small, hypodense masses, often attached to the valve leaflets by a short pedicle. The aortic and mitral valves are the most commonly affected. They may be difficult to detect on CMR due to their small size, but typically appear isointense on T1-weighted images and hyperintense on T2-weighted images. Surrounding turbulent flow may be seen on cine images and may be the only abnormality evident if the mass is too small to visualize. Surgical excision is recommended for left sided tumors, for lesions > 1 cm, or for symptomatic cases (cerebral embolic events or angina from coronary ostial obstruction).

The primary differential considerations for valvular pathology include thrombus and vegetation, both of which are more frequently encountered. Thrombus may be difficult to distinguish from a papillary fibroelastoma, but may be differentiated by its signal characteristics and lack of contrast enhancement, if large enough to reliably assess. The appearances of thrombus are discussed separately below, although, unlike a papillary fibroelastoma, thrombus may demonstrate high T1-weighted signal if acute or subacute, or low T2-weighted signal if subacute or chronic [30]. Vegetation usually arises from the tips of the valve leaflets, is not attached by a stalk, is associated with a greater degree of valvular destruction, and often occurs in the context of suspected endocarditis.

Rhabdomyoma

Rhabdomyomas are the most common primary cardiac neoplasm of infancy and childhood [31, 32]. They typically present within the first year of life with a mean age at diagnosis of 2 weeks. Males are more commonly affected than females and 80–90% of cases are seen in the context of tuberous sclerosis [33, 34]. Derived from striated muscle cells, they are microscopically considered to be hamartomas [3]. Macroscopically, they are well-circumscribed masses arising within the myocardium and are multiple in up to 90% of cases.

On CT, they appear as hypodense intramural masses ranging from a few millimeters to several centimeters. They are usually confined to the myocardium but may rarely project into the ventricle [35]. On CMR, they appear isointense to myocardium on T1-weighted images and hyperintense on T2-weighted images [36, 37]. They typically demonstrate minimal to no contrast enhancement.

Most remain asymptomatic and spontaneously regress in early childhood without the need for surgical intervention [38]. Surgery is considered in cases of hemodynamic compromise or refractory arrhythmias.

Fibroma

Fibromas are the second most common primary cardiac neoplasm of childhood presenting at a mean age of 11 years [39]. Like rhabdomyomas, they also arise in an intramural location, typically within the left ventricle or interventricular septum [40]. However, in contrast to rhabdomyomas, fibromas are usually solitary. Histologically, they are composed of neoplastic fibroblasts interspersed with large amounts of collagen. Associations include familial adenomatous polyposis, Gardner syndrome, and several developmental anomalies including cleft lip and cleft palate [41].

On CT, fibromas appear as well-defined intramural masses of soft-tissue attenuation and may contain coarse dystrophic calcification, which can help distinguish them from rhabdomyomas. On CMR, fibromas appear isointense to

myocardium on T1-weighted images and hypointense on T2-weighted images [42, 43]. Signal intensity is usually homogenous unless calcification is present, which may give rise to central areas of low signal. Fibromas are avascular and therefore do not enhance during first pass perfusion imaging. However, they classically display intense late gadolinium enhancement at 7–10 min owing to their large extracellular component, which allows gadolinium to diffuse into and remain within the interstitial space but not across cell membranes [36].

Hemangioma

Cardiac hemangiomas, also known as cardiac venous malformations, are rare lesions accounting for 5–10% of primary cardiac tumors [3]. They consist of endothelial-lined channels and may be divided into capillary, cavernous, or arteriovenous subtypes. They are usually solitary lesions and are typically found in the ventricles, although they may arise in any cardiac chamber [44].

On non-contrast-enhanced CT, they appear as heterogenous masses and may contain foci of calcification. On CMR, they appear hyperintense on both T1- and T2-weighted sequences due to slow flow and often contain hypointense fibrous septae [36, 45]. Avid enhancement is characteristic and reflects the vascular nature of the mass [45].

Malignant Masses

Cardiac Sarcoma

Primary cardiac malignancies are uncommon accounting for 25% of primary cardiac tumors. Sarcomas represent the vast majority (95%) of such cases, with primary cardiac lymphomas and pericardial mesotheliomas accounting for the remainder [3].

Sarcomas may occur at any age but typically present in the third to fifth decade of life. Mean age at diagnosis is 41 years. Dyspnea and orthopnea are the most common presenting symptoms and are often due to pulmonary venous hypertension and pulmonary edema. Prognosis is very poor, with mean survival ranging from 9.6 to 16.5 months [46–48]. Complete surgical resection with negative margins is necessary for optimal survival. A 17-year retrospective study found that patients who underwent surgery had a mean survival of 12 months compared with a mean survival of 1 month for those who did not undergo surgery [49]. A Mayo Clinic review of 24 patients who underwent surgery over a 32-year period found that mean survival was extended to 17 months for patients who underwent an R0 resection (i.e., microscopically negative margins) compared with 6 months following an R1 resection (i.e., macroscopically negative but microscopically positive margins) [50]. These findings serve to highlight the importance of accurate preoperative imaging, particularly regarding the margins of the mass and the extent of local invasion.

Undifferentiated sarcomas usually originate in the left atrium and may invade and occlude the pulmonary veins and left atrial appendage [51]. Pulmonary vein involvement often necessitates a pneumonectomy and is considered a contraindication to surgery by some surgeons. Macroscopically, they may appear as either focal intracavitary lesions or diffuse infiltrative masses with central areas of necrosis and hemorrhage. Angiosarcomas typically demonstrate similar aggressive appearances to undifferentiated sarcoma and may also present as a low-attenuation intracavitary mass or as an infiltrative mass invading the myocardium and pericardium [52]. However, unlike undifferentiated sarcomas, angiosarcomas usually arise in the right atrium, right ventricle or, less commonly, the pericardium or pulmonary arteries [49, 53] (Fig. 1). Encasement and invasion of the right coronary artery is not uncommon and may necessitate a coronary resection and replacement if surgical management is being considered.

Rhabdomyosarcomas represent 4–7% of cardiac sarcomas and are the most common cardiac malignancy in infants and children [3, 33]. Unlike undifferentiated sarcomas and angiosarcomas, rhabdomyosarcomas demonstrate no predilection for any specific chamber. Similar to rhabdomyomas, multiple sites of origin are not uncommon [54, 55]. On CT, rhabdomyosarcomas appear as large infiltrative masses that may surround central areas of necrosis. On CMR, they appear isointense to myocardium on T1-weighted images and hyperintense on T2-weighted images. Enhancement is typically homogenous, although central areas of necrosis may give rise to central areas hypoenhancement [18, 36].

The remainder of the cardiac sarcomas are extremely rare and include osteosarcoma, fibrosarcoma, liposarcoma, and leiomyosarcoma. Osteosarcomas often contain dense calcification and virtually always arise in the left atrium producing signs and symptoms of congestive cardiac failure [56]. Leiomyosarcomas also has a predilection for the left atrium, usually arising from the posterior wall, although it may also arise in the smooth muscle of the pulmonary arteries and veins and spread to involve the heart.

Primary Cardiac Lymphoma

Primary cardiac lymphoma is rare accounting for < 5% of primary cardiac malignancies. Cardiac involvement of extracardiac lymphomas is far more common. Almost all primary cardiac lymphomas are aggressive B cell lymphomas and usually occur in immunocompromised patients, such as those with HIV or transplant recipients on long term immunosuppressants [57]. Like other primary cardiac malignancies,

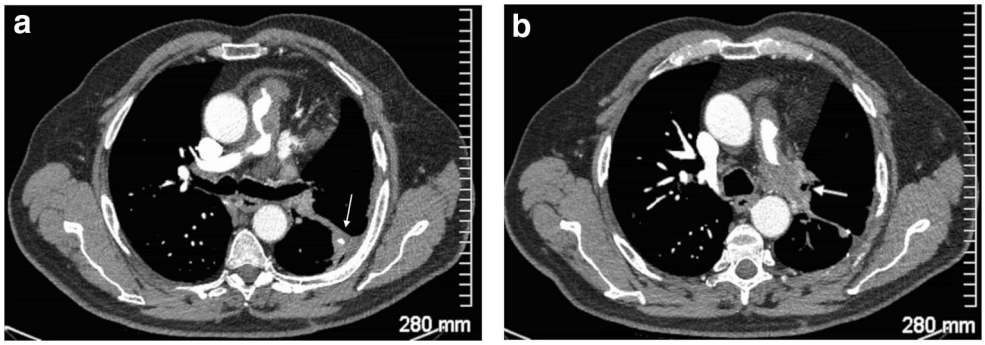

Fig. 1 Angiosarcoma. **a** Axial contrast-enhanced CT showing nodular thickening of the pulmonary trunk and right ventricular outflow tract. A partially calcified, left lower lobe pulmonary metastasis is also present (arrow). **b** Axial contrast-enhanced CT showing occlusion of the left main pulmonary artery and encasement of the left upper lobe bronchus (arrow) by an invasive soft tissue mass

prognosis is poor although remission has been reported in cases of early diagnosis and chemotherapy [58].

Primary cardiac lymphoma usually arises in the right side of the heart, most commonly in the right atrium, and often infiltrates the pericardium resulting in a pericardial effusion [59, 60] (Fig. 2). Extensive nodular infiltration of the myocardium is also often present at the time of diagnosis [61]. Epicardial extension along the surface of the heart and encasement of the aortic root and coronary arteries have been described [62].

The imaging appearances of primary and secondary cardiac lymphoma are similar, usually manifesting as a homogenous isointense mass on T1- and T2-weighted sequences [63]. Central areas of necrosis and hemorrhage often seen in other cardiac malignances are rarely seen in cardiac lymphoma, which may serve as a useful discriminating feature [64].

Cardiac Metastases

Cardiac metastases represent the most common cardiac tumors and are 20–40 times more common than primary cardiac neoplasms [65]. They are typically asymptomatic but are discovered at autopsy in 10–12% of patients with a known malignancy [66]. Melanoma is perhaps the only primary tumor with a tendency for cardiac spread and can involve the myocardium in up to 50% of cases [67]. Other sites of origin include lung, breast, and esophageal carcinoma as well as lymphoma and leukemia [68].

Four routes of spread are described: hematogenous dissemination, lymphatic spread, venous extension and direct invasion. Hematogenous dissemination usually results in myocardial deposits and is typically seen with melanoma, lymphoma, or leukemia. Lymphatic spread is usually the result of retrograde propagation through the mediastinal lymphatics and results in cancerous cells implanting on the epicardium or pericardium [1]. Thoracic malignancies, in particular lung and breast carcinomas, account for the majority of such cases. Venous extension describes tumors propagating along the veins leading to the heart. Infradiaphragmatic tumors may ascend along the IVC and involve the right atrium [69]. Renal cell carcinoma is the typical example, but hepatocellular and adrenocortical carcinoma may also spread via this route. Lastly, direct extension is usually seen in thoracic malignancies due to their proximity to the heart and is most commonly the result of lung, breast or esophageal carcinoma or, less commonly, pleural mesothelioma.

On CT, cardiac metastases appear as solid enhancing nodules or masses [30]. The margins of the mass may be well-defined or infiltrative. On CMR, cardiac metastases do not have any specific appearances but usually appear hypointense on T1-weighted images and hyperintense on T2-weighted images. Melanoma is an exception usually appearing hyperintense on T1-weighted images due to the presence of melanin [67, 70].

Pericardial metastases may present as pericardial thickening, nodularity, or a pericardial effusion. Malignant pericardial effusions are typically exudative and often hemorrhagic, and thus appear denser on CT and more hyperintense on T1-weighted CMR images compared with simple transudative effusions.

Pseudotumors

Thrombus

Once a cardiac mass is identified, thrombus should be the first consideration as it is the most common cardiac mass and can be fatal if left untreated [71]. It can occur in any cardiac chamber but most commonly affects the left side of the heart. It is usually caused by atrial fibrillation, wall motion of abnormalities from prior myocardial infarction, indwelling catheters or devices, or hypercoagulable states.

In the left atrium, thrombus usually forms in the setting of atrial fibrillation and is typically located against the posterior wall or within the left atrial appendage. CT is highly sensitive at detecting thrombus within the left atrial appendage but has a lower specificity as circulatory stasis may mimic a true filling

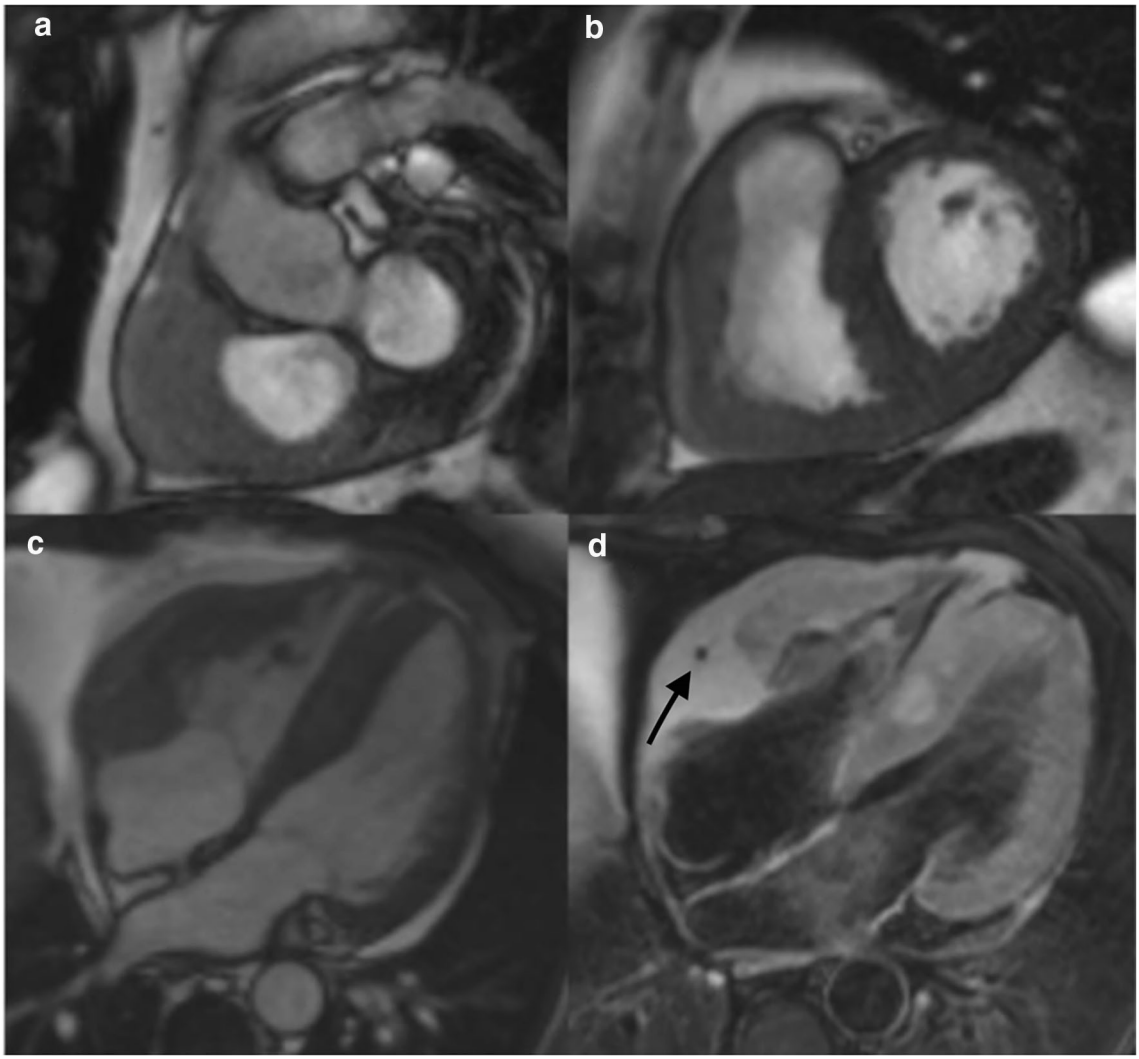

Fig. 2 Primary cardiac lymphoma. **a** Balanced steady-state gradient recall echo sequence (True FISP). Basal short axis slice showing extension of primary cardiac lymphoma around the right ventricle. **b** Mid ventricular slice showing involvement of the right ventricular free wall and inferior wall. **c** Four-chamber view confirming infiltration of the right atrium, right ventricular free wall, and interventricular septum. **d** T2-weighted fast spin echo sequence. Four-chamber view showing encasement of the right coronary artery (arrow) (credit: Dr. Jessica Webb, Consultant Cardiologist, Guys and Thomas Hospital, UK)

defect [72, 73]. Specificity however can be improved by performing an additional delayed phase. A 2015 meta-analysis reported a pooled sensitivity and specificity of 99.1% and 98.9%, respectively, when delayed-imaging, ECG-gating and heart rate control were performed [74]. Similarly, a 2018 meta-analysis assessing CMR in the detection of left atrial and left atrial appendage thrombus reported a pooled sensitivity and specificity of 100% and 99% if delayed enhancement sequences were acquired [75•].

In the left ventricle, thrombus typically forms in areas of myocardial hypokinesis or within left ventricular aneurysms, which are usually due to prior myocardial infarction. Left ventricular thrombus usually has a crescentic morphology with a broad attachment to the ventricular wall, although pedunculated thrombi mimicking myxomas have been reported [76].

In the right ventricle, thrombus typically forms around indwelling central venous catheters or conduction leads, but has also been described in the setting of arrhythmogenic right ventricular dysplasia, systemic lupus erythematosus, Behcet's disease, metastases, and trauma [69, 77].

On CT, thrombus appears as an intracavitary filling defect [78]. Foci of calcification may be seen in chronic thrombus. On CMR, the signal characteristics of thrombus depend on its age. In the acute setting, thrombus is composed of oxygenated hemoglobin and demonstrates intermediate signal intensity on T1- and T2-weighted images. As it ages, oxyhemoglobin in converted to methemoglobin, shortening the T1 and T2 relaxation times and leading to increased signal on T1-weighted sequences and decreased signal on T2-weighed sequences [79]. Hence, subacute thrombus appears hyperintense on T1-weighted sequences and hypointense on T2-weighted

sequences. After a further period of time, thrombus is eventually replaced by fibrous tissue and becomes water-deplete leading to low signal intensity on T1- and T2-weighted images.

Contrast-enhanced CMR is the most accurate way of distinguishing between thrombus and a true neoplasm. Thrombus lacks a blood supply and will not enhance on post-contrast sequences. Rarely, however, chronic thrombus may show mild peripheral enhancement due to its fibrous content. [69]

Pericardial Cyst

Pericardial cysts are benign, congenital, fluid-filled lesions, most commonly located in the right cardiophrenic angle [80]. Their typical location helps distinguish them from other cystic mediastinal abnormalities such as bronchogenic, thymic, and foregut duplication cysts. They are almost always asymptomatic but rare cases have been reported of large cysts causing hemodynamic compromise, or hemorrhage into a cyst leading it to exert mass effect.

On CT, pericardial cysts appear as thin-walled, fluid-density structures which do not communicate with the pericardial space (unlike pericardial diverticulae) and do not enhance post-contrast. On CMR, they demonstrate homogenous low signal on T1-weighted images and very high signal on T2-weighted images, as would be expected of a simple cyst [81].

Pre-op 3D Reconstruction and Planning

Advances in multidetector CT hardware and more sophisticated post-processing algorithms have made 3D reconstructions a useful adjunct in the assessment of a cardiac mass [82]. Both maximum intensity projection (MIP) and volume rendering (VR) can be used for reconstructing CT datasets and can assist in displaying information that can be difficult to appreciate on two-dimensional (2D) images.

MIP images are reconstructed by selecting the highest attenuation voxels in a given volume and displaying them as a single 2D image. MIP images are optimized for evaluating vascular anatomy and can be of value in assessing the course and locations of the coronary arteries and their relationship to the mass. Volume rendering employs a more complex algorithm and allows for better visualization of soft tissues, bony structures, and vasculature in a single image. In VR, each voxel is assigned a color and transparency based on its attenuation and the information is displayed as a single image which can be manipulated to better understand the anatomic and spatial relationships between the margins of the mass and the surrounding structures.

Cinematic rendering is a novel technique which is similar to VR but incorporates a more complex lighting model to create more photorealistic images. It has not been widely studied and is not widely available but it has shown promise in several applications, including cardiac imaging. [83–85] Rowe et al. published a case of a spindle cell sarcoma of the right ventricle illustrating how cinematic rendering can be used to demarcate the margins and extent of the mass [84].

Three-Dimensional Printed Models

Three-dimensional printed models are an emerging technology which have been incorporated into cardiology and cardiac surgery in recent years [86, 87]. 3D printing is a form of additive manufacturing in which personalized 3D models are created from digital images by the layer-on-layer addition of new material to an existing surface. While its use in the setting of cardiac masses is still largely experimental, a substantial literature supports the benefit of 3D printing in patients with congenital heart disease. [88–90] The Radiological Society of North America 3D Printing Special Interest Group has recently published guidelines outlining the specific scenarios in which 3D printing is appropriate, with truncus arteriosus, double outlet right ventricle and double outlet left ventricle scoring highest on their appropriateness rating [91].

Although still in its infancy, the field is advancing at a rapid pace and several reports have now been published describing the use of 3D models in the preoperative planning of a cardiac mass, including cases of a poorly differentiated sarcoma infiltrating the tricuspid valve, a right ventricular fibroma, a left atrial osteosarcoma and renal cell carcinoma metastatic to the right atrium [92–94]. In such cases, the additional value in a 3D model over a 3D reconstructed image has been largely attributed to easier visualization of the margins of the mass and a better appreciation of the relationship between the mass and the surrounding structures.

Surgeons' initial experiences with 3D printed models have been largely positive. In one study, 4/5 surgeons found the models helpful in potentially reducing surgical complications and all five reported that they would recommend it to a colleague [95].

Conclusion

With the widespread and routine use of echocardiography and CT, the incidental detection of a cardiac mass is not uncommon. CT and CMR are complementary tools in the diagnosis and preoperative assessment of a cardiac mass. CMR provides superior tissue characterization, whereas CT better depicts calcification and has

superior spatial resolution allowing for precise anatomic localization and detailed preoperative planning. Knowledge of the epidemiology and typical appearances of the most common cardiac masses is now mandatory for radiologists and cardiologists reporting cardiac imaging and facilitates optimal patient management. 3D reconstructions are a valuable adjunct in the preoperative assessment of a cardiac mass and may allow for a better appreciation of the margins of the mass and its relationship with surrounding structures. 3D printing is an emerging technology which has recently been incorporated into the management of complex congenital heart disease and may be of additional value in selected patients with a cardiac mass.

Compliance with Ethical Standards

Conflict of Interest Stephen Liddy, Colin McQuade, Kevin P. Walsh, Bryan Loo, and Orla Buckley declare that they have no conflict of interest.

Human and Animal Rights and Informed Consent This article does not contain any studies with human or animal subjects performed by any of the authors.

References

Papers of particular interest, published recently, have been highlighted as:
- • Of importance
- •• Of major importance

1. Lam KY, Dickens P, Chan ACL. Tumors of the heart: a 20-year experience with a review of 12 485 consecutive autopsies. Arch Pathol Lab Med. 1993.Oct;117(10):1027-31.
2. Sütsch G, Jenni R, von Segesser L, Schneider J. Heart tumors: incidence, distribution, diagnosis. Exemplified by 20,305 echocardiographies. Schweiz Med Wochenschr. 1991.Apr;121(17):621–9.
3. Mc Allister HA. Primary tumors and cysts of the heart and pericardium. Curr Probl Cardiol. 1979;4:1–51. https://doi.org/10.1016/0146-2806(79)90008-2.
4. Elbardissi AW, Dearani JA, Daly RC, Mullany CJ, Orszulak TA, Puga FJ, et al. Survival after resection of primary cardiac tumors: a 48-year experience. Circulation. 2008;118:S7–S15. https://doi.org/10.1161/CIRCULATIONAHA.107.783126.
5. Roberts WC. Primary and secondary neoplasms of the heart. Am J Cardiol. 1997;80:671–82. https://doi.org/10.1016/S0002-9149(97)00587-0.
6. Taguchi S. Comprehensive review of the epidemiology and treatments for malignant adult cardiac tumors. Gen Thorac Cardiovasc Surg. 2018;66:257–62.https://doi.org/10.1007/s11748-018-0912-3.
7. Junttila MJ, Fishman JE, Lopera GA, Pattany PM, Velazquez DL, Williams AR, et al. Safety of serial MRI in patients with implantable cardioverter defibrillators. Heart. 2011;97:1852–6. https://doi.org/10.1136/heartjnl-2011-300153.
8. Kakouros N, Giles J, Crundwell NB, McWilliams ET. The utility of cardiac CT beyond the assessment of suspected coronary artery disease. Clin Radiol. 2012 Jul;67(7):695-708. https://doi.org/10.1016/j.crad.2011.11.011.
9. Achenbach S, Kondo T. Technical advances in cardiac CT. Cardiol Clin. 2012;30:1–8. https://doi.org/10.1016/j.ccl.2011.11.002.
10. Cody DD, Mahesh M. AAPM/RSNA physics tutorial for residents: technologic advances in multidetector CT with a focus on cardiac imaging. Radiographics. 2007;27:1829–37. https://doi.org/10.1148/rg.276075120.
11. Yin WH, Lu B, Li N, Han L, Hou ZH, Wu RZ, et al. Iterative reconstruction to preserve image quality and diagnostic accuracy at reduced radiation dose in coronary CT angiography: an intraindividual comparison. JACC Cardiovasc Imaging. 2013;6:1239–49. https://doi.org/10.1016/j.jcmg.2013.08.008.
12. Fuchs TA, Stehli J, Bull S, Dougoud S, Clerc OF, Herzog BA, et al. Coronary computed tomography angiography with model-based iterative reconstruction using a radiation exposure similar to chest X-ray examination. Eur Heart J. 2014;35:1131–6. https://doi.org/10.1093/eurheartj/ehu053.
13. • Kassi M, Polsani V, Schutt RC, Wong S, Nabi F, Reardon MJ, et al. Differentiating benign from malignant cardiac tumors with cardiac magnetic resonance imaging. J Thorac Cardiovasc Surg. 2019;**157**:**1912–1922.e2**. https://doi.org/10.1016/j.jtcvs.2018.09.057. **This study represents one of the largest reported experiences, and the largest prospective cohort study, evaluating the utility of contemporary CMR is differentiating benign and malignant cardiac tumors**.
14. Patel RD, Lim RP, Axel L, Srichai MB. Diagnostic utility of cardiac MRI in clinical evaluation of cardiac masses with histopathological correlation. J Cardiovasc Magn Reson. 2013;14. https://doi.org/10.1186/1532-429x-14-s1-p298.
15. Tumma R, Dong W, Wang J, Litt H, Han Y. Evaluation of cardiac masses by CMR—strengths and pitfalls: a tertiary center experience. Int J Cardiovasc Imaging. 2016;32:913–20. https://doi.org/10.1007/s10554-016-0845-9.
16. Patel R, Lim RP, Saric M, Nayar A, Babb J, Ettel M, et al. Diagnostic performance of cardiac magnetic resonance imaging and echocardiography in evaluation of cardiac and Paracardiac masses. Am J Cardiol. 2016;117:135–40. https://doi.org/10.1016/j.amjcard.2015.10.014.
17. Rathi VK, Czajka AT, Thompson DV, Doyle M, Tewatia T, Yamrozik J, et al. Can cardiovascular MRI be used to more definitively characterize cardiac masses initially identified using echocardiography? Echocardiography. 2018;35:735–42.
18. Grebenc ML, Rosado de Christenson ML, Burke AP, Green CE, Galvin JR. Primary cardiac and pericardial neoplasms: radiologic-pathologic correlation. RadioGraphics. 2013;20:1073–103. https://doi.org/10.1148/radiographics.20.4.g00jl081073.
19. Carney JA. Differences between nonfamilial and familial cardiac myxoma. Am J Surg Pathol. 1985;9:53–5. https://doi.org/10.1097/00000478-198501000-00009.
20. Shetty Roy AN, Radin M, Sarabi D, Shaoulian E. Familial recurrent atrial myxoma: Carney's complex. Clin Cardiol. 2011. https://doi.org/10.1002/clc.20845 LK - http://sfx.library.uu.nl/utrecht?sid=EMBASE&issn=01609289&id=doi:10.1002%2Fclc.20845&atitle=Familial+recurrent+atrial+myxoma%3A+Carney%27s+complex&stitle=Clin.+Cardiol.&title=Clinical+Cardiology&volume=34&issue=2&spage=83&epage=86&aulast=Roy&aufirst=A.+Nagesh+Shetty&auinit=A.N.S.&aufull=Roy+A.N.S.&coden=CLCAD&isbn=&pages=83-86&date=2011&auinit1=A&auinitm=N.S.
21. Colin GC, Gerber BL, Amzulescu M, Bogaert J. Cardiac myxoma: a contemporary multimodality imaging review. Int J Cardiovasc Imaging. 2018;34:1789–808. https://doi.org/10.1007/s10554-018-1396-z.
22. Wei K, Guo HW, Fan SY, Sun XG, Hu SS. Clinical features and surgical results of cardiac myxoma in Carney complex. J Card Surg. 2019;34:14–9. https://doi.org/10.1111/jocs.13980.

23. Hananouchi GI, Goff WB. Cardiac lipoma: six-year follow-up with MRI characteristics, and a review of the literature. Magn Reson Imaging. 1990;8:825–8. https://doi.org/10.1016/0730-725X(90)90021-S.
24. Heyer CM, Kagel T, Lemburg SP, Bauer TT, Nicolas V. Lipomatous hypertrophy of the interatrial septum: a prospective study of incidence, imaging findings, and clinical symptoms. Chest. 2003;124:2068–73. https://doi.org/10.1378/chest.124.6.2068.
25. Fan CM, Fischman AJ, Kwek BM, Abbara S, Aquino SL. Lipomatous hypertrophy of the interatrial septum: increased uptake on FDG PET. Am J Roentgenol. 2005;184:339–42. https://doi.org/10.2214/ajr.184.1.01840339.
26. Tazelaar HD, Locke TJ, McGregor CGA. Pathology of surgically excised primary cardiac tumors. Mayo Clin Proc. 1992;67:957–65. https://doi.org/10.1016/S0025-6196(12)60926-4.
27. Georghiou GP, Vidne BA, Sahar G, Sharoni E, Fuks A, Porat E. Primary cardiac valve tumors. Asian Cardiovasc Thorac Ann. 2010;18:226–8. https://doi.org/10.1177/0218492310367522.
28. Howard RA, Aldea GS, Shapira OM, Kasznica JM, Davidoff R. Papillary fibroelastoma: increasing recognition of a surgical disease. Ann Thorac Surg. 1999;68:1881–5. https://doi.org/10.1016/S0003-4975(99)00860-7.
29. Carino D, Nicolini F, Molardi A, Indira Dadamo C, Gherli T. Unusual Locations for Cardiac Papillary Fibroelastomas. J Heart Valve Dis. 2017 Mar;26(2):226-230.
30. Motwani M, Kidambi A, Herzog BA, Uddin A, Greenwood JP, Plein S. MR imaging of cardiac tumors and masses: a review of methods and clinical applications. Radiology. 2013;268:26–43.
31. Ying L, Lin R, Gao Z, Qi J, Zhang Z, Gu W. Primary cardiac tumors in children: a center's experience. J Cardiothorac Surg. 2016;11:52. https://doi.org/10.1186/s13019-016-0448-5.
32. Delmo Walter EM, Javier MF, Sander F, Hartmann B, Ekkernkamp A, Hetzer R. Primary cardiac tumors in infants and children: surgical strategy and long-term outcome. Ann Thorac Surg. 2016;102:2062–9. https://doi.org/10.1016/j.athoracsur.2016.04.057.
33. Beghetti M, Gow RM, Haney I, Mawson J, Williams WG, Freedom RM. Pediatric primary benign cardiac tumors: a 15-year review. Am Heart J. 1997;134:1107–14. https://doi.org/10.1016/S0002-8703(97)70032-2.
34. Bosi G, Lintermans JP, Pellegrino PA, Svaluto-Moreolo G, Vliers A. The natural history of cardiac rhabdomyoma with and without tuberous sclerosis. Acta Paediatr Int J Paediatr. 1996;85:928–31. https://doi.org/10.1111/j.1651-2227.1996.tb14188.x.
35. Restrepo CS, Largoza A, Lemos DF, Diethelm L, Koshy P, Castillo P, et al. CT and MR imaging findings of benign cardiac tumors. Curr Probl Diagn Radiol. 2005;34:12–21. https://doi.org/10.1067/j.cpradiol.2004.10.002.
36. Kiaffas MG, Powell AJ, Geva T. Magnetic resonance imaging evaluation of cardiac tumor characteristics in infants and children. Am J Cardiol. 2002;89:1229–33. https://doi.org/10.1016/S0002-9149(02)02314-7.
37. Berkenblit R, Spindola-Franco H, Frater RWM, Fish BB, Glickstein JS. MRI in the evaluation and management of a newborn infant with cardiac rhabdomyoma. Ann Thorac Surg. 1997;63:1475–7. https://doi.org/10.1016/S0003-4975(97)00113-6.
38. Smythe JF, Dyck JD, Smallhorn JF, Freedom RM. Natural history of cardiac rhabdomyoma in infancy and childhood. Am J Cardiol. 1990;66:1247–9. https://doi.org/10.1016/0002-9149(90)91109-J.
39. Burke A, Tavora F. The 2015 WHO classification of tumors of the heart and pericardium. J Thorac Oncol. 2016;11:441–52. https://doi.org/10.1016/j.jtho.2015.11.009.
40. Nwachukwu H, Li A, Nair V, Nguyen E, David TE, Butany J. Cardiac fibroma in adults. Cardiovasc Pathol. 2011;20:e146–52. https://doi.org/10.1016/j.carpath.2010.08.006.
41. de León GA, Zaeri N, Donner RM, Karmazin N. Cerebral rhinocele, hydrocephalus, and cleft lip and palate in infants with cardiac fibroma. J Neurol Sci. 1990;99:27–36. https://doi.org/10.1016/0022-510X(90)90196-T.
42. Hoffmann U, Globits S, Schima W, Loewe C, Puig S, Oberhuber G, et al. Usefulness of magnetic resonance imaging of cardiac and paracardiac masses. Am J Cardiol. 2003;92:890–5. https://doi.org/10.1016/S0002-9149(03)00911-1.
43. Luna A, Ribes R, Caro P, Vida J, Erasmus JJ. Evaluation of cardiac tumors with magnetic resonance imaging. Eur Radiol. 2005;15:1446–55. https://doi.org/10.1007/s00330-004-2603-y.
44. Li W, Teng P, Xu H, Ma L, Ni Y. Cardiac hemangioma: a comprehensive analysis of 200 cases. Ann Thorac Surg. 2015;99:2246–52. https://doi.org/10.1016/j.athoracsur.2015.02.064.
45. Oshima H, Hara M, Kono T, Shibamoto Y, Mishima A, Akita S. Cardiac hemangioma of the left atrial appendage: CT and MR findings. J Thorac Imaging. 2003;18:204–6. https://doi.org/10.1097/00005382-200307000-00012.
46. Truong PT, Jones SO, Martens B, Alexander C, Paquette M, Joe H, et al. Treatment and outcomes in adult patients with primary cardiac sarcoma: the British Columbia Cancer Agency experience. Ann Surg Oncol. 2009;16:3358–65. https://doi.org/10.1245/s10434-009-0734-8.
47. Donsbeck AV, Ranchere D, Coindre JM, Le Gall F, Cordier JF, Loire R. Primary cardiac sarcomas: an immunohistochemical and grading study with long-term follow-up of 24 cases. Histopathology. 1999;34:295–304. https://doi.org/10.1046/j.1365-2559.1999.00636.x.
48. Bakaeen FG, Reardon MJ, Coselli JS, Miller CC, Howell JF, Lawrie GM, et al. Surgical outcome in 85 patients with primary cardiac tumors. Am J Surg. 2003;186:641–7. https://doi.org/10.1016/j.amjsurg.2003.08.004.
49. Hamidi M, Moody JS, Weigel TL, Kozak KR. Primary cardiac sarcoma. Ann Thorac Surg. 2010;90:176–81. https://doi.org/10.1016/j.athoracsur.2010.03.065.
50. Simpson L, Kumar SK, Okuno SH, Schaff HV, Porrata LF, Buckner JC, et al. Malignant primary cardiac tumors: review of a single institution experience. Cancer. 2008;112:2440–6. https://doi.org/10.1002/cncr.23459.
51. Perchinsky MJ, Lichtenstein SV, Tyers GFO. Primary cardiac tumors: forty years' experience with 71 patients. Cancer. 1997;79:1809–15. https://doi.org/10.1002/(SICI)1097-0142(19970501)79:9<1809::AID-CNCR25>3.0.CO;2-0.
52. Buckley O, Madan R, Kwong R, Rybicki FJ, Hunsaker A. Cardiac masses, part 2: key imaging features for diagnosis and surgical planning. Am J Roentgenol. 2011;197:W842–51. https://doi.org/10.2214/AJR.11.6903.
53. Burnside N, MacGowan SW. Malignant primary cardiac tumours. Interact Cardiovasc Thorac Surg. 2012;15:1004–6. https://doi.org/10.1093/icvts/ivs350.
54. Shapiro LM. General cardiology: cardiac tumours: diagnosis and management. Heart. 2002;85:218–22. https://doi.org/10.1136/heart.85.2.218.
55. Villacampa VM, Villarreal M, Ros LH, Álvarez R, Cózar M, Fuertes MI. Cardiac rhabdomyosarcoma: diagnosis by MR imaging. Eur Radiol. 1999;9:634–7. https://doi.org/10.1007/s003300050723.
56. Burke A, Jeudy J, Virmani R. Cardiac tumours: an update. Heart. 2008;94:117–23. https://doi.org/10.1136/hrt.2005.078576.
57. Holladay AO, Siegel RJ, Schwarfz DA. Cardiac malignant lymphoma in acquired immune deficiency syndrome. Cancer. 1992;70:2203–7. https://doi.org/10.1002/1097-0142(19921015)70:8<2203::AID-CNCR2820700831>3.0.CO;2-6.
58. Ceresoli GL, Ferreri AJM, Bucci E, Ripa C, Ponzoni M, Villa E. Primary cardiac lymphoma in immunocompetent patients: diagnostic and therapeutic management. Cancer. 1997;80:1497–506.

https://doi.org/10.1002/(SICI)1097-0142(19971015)80:8<1497::AID-CNCR18>3.0.CO;2-0.
59. Perrone MA, Intorcia A, Morgagni R, Marchei M, Sergi D, Pugliese L, et al. Primary cardiac lymphoma: the role of multimodality imaging. J Cardiovasc Med. 2018:1. https://doi.org/10.2459/JCM.0000000000000668.
60. Coulier B, Colin GC, Tourmous H, Floris N, Van Eeckhout P, Scavée C. Imaging features of primary cardiac lymphoma. Diagn Interv Imaging. 2018;99:115–7. https://doi.org/10.1016/j.diii.2017.05.013.
61. Petrich A, Cho SI, Billett H. Primary cardiac lymphoma: an analysis of presentation, treatment, and outcome patterns. Cancer. 2011;117:581–9. https://doi.org/10.1002/cncr.25444.
62. Jeudy J, Kirsch J, Tavora F, Burke AP, Franks TJ, Mohammed TL, et al. From the radiologic pathology archives: cardiac lymphoma: radiologic-pathologic correlation. RadioGraphics. 2012;32:1369–80. https://doi.org/10.1148/rg.325115126.
63. Carter BW, Wu CC, Khorashadi L, Godoy MCB, De Groot PM, Abbott GF, et al. Multimodality imaging of cardiothoracic lymphoma. Eur J Radiol. 2014;83:1470–82. https://doi.org/10.1016/j.ejrad.2014.05.018.
64. Dorsay TA, Ho VB, Rovira MJ, Armstrong MA, Brissette MD. Primary cardiac lymphoma: CT and MR findings. J Comput Assist Tomogr. 1993;17:978–81. https://doi.org/10.1097/00004728-199311000-00025.
65. Butany J, Nair V, Naseemuddin A, Nair GM, Catton C, Yau T. Cardiac tumours: diagnosis and management. Lancet Oncol. 2005;6:219–28. https://doi.org/10.1016/S1470-2045(05)70093-0.
66. Abraham KP, Reddy V, Gattuso P. Neoplasms metastatic to the heart: review of 3314 consecutive autopsies. bAm J Cardiovasc Pathol 1990;3(3):195-8.
67. Mousseaux E, Meunier P, Azancott S, Dubayle P, Gaux JC. Cardiac metastatic melanoma investigated by magnetic resonance imaging. Magn Reson Imaging. 1998;16:91–5. https://doi.org/10.1016/S0730-725X(97)00200-2.
68. Lichtenberger JP, Reynolds DA, Keung J, Keung E, Carter BW. Metastasis to the heart: a radiologic approach to diagnosis with pathologic correlation. Am J Roentgenol. 2016;207:764–72. https://doi.org/10.2214/AJR.16.16148.
69. Kim EY, Choe YH, Sung K, Park SW, Kim JH, Ko YH. Multidetector CT and MR imaging of cardiac tumors. Korean J Radiol. 2009;10:164. https://doi.org/10.3348/kjr.2009.10.2.164.
70. Crean AM, Juli C. Diagnosis of metastatic melanoma to the heart with an intrinsic contrast approach using melanin inversion recovery imaging. J Comput Assist Tomogr. 2007;31:924–30. https://doi.org/10.1097/RCT.0b013e31804b213b.
71. Kim DH, Il Choi S, Choi JA, Chang HJ, Choi DJ, Lim C, et al. Various findings of cardiac thrombi on MDCT and MRI. J Comput Assist Tomogr. 2006;30:572–7. https://doi.org/10.1097/00004728-200607000-00004.
72. Hur J, Kim YJ, Lee HJ, Nam JE, Ha JW, Heo JH, et al. Dual-enhanced cardiac CT for detection of left atrial appendage thrombus in patients with stroke: a prospective comparison study with transesophageal echocardiography. Stroke. 2011;42:2471–7. https://doi.org/10.1161/STROKEAHA.110.611293.
73. Hur J, Pak HN, Kim YJ, Lee HJ, Chang HJ, Hong YJ, et al. Dual-enhancement cardiac computed tomography for assessing left atrial thrombus and pulmonary veins before radiofrequency catheter ablation for atrial fibrillation. Am J Cardiol. 2013;112:238–44. https://doi.org/10.1016/j.amjcard.2013.03.018.
74. Zou H, Zhang Y, Tong J, Liu Z. Multidetector computed tomography for detecting left atrial/left atrial appendage thrombus: a meta-analysis. Intern Med J. 2015;45:1044–53. https://doi.org/10.1111/imj.12862.
75.• Chen J, Zhang H, Zhu D, Wang Y, Byanju S, Liao M. Cardiac MRI for detecting left atrial/left atrial appendage thrombus in patients with atrial fibrillation : meta-analysis and systematic review. Herz. 2018. https://doi.org/10.1007/s00059-017-4676-9. **This study represents a comprehensive systematic review and meta-analysis evaluating contemporary CMR in detecting left atrial appendage thrombus and compares the accuracy of various imaging sequences**.
76. Scheffel H, Baumueller S, Stolzmann P, Leschka S, Plass A, Alkadhi H, et al. Atrial myxomas and thrombi: comparison of imaging features on CT. Am J Roentgenol. 2009;192:639–45. https://doi.org/10.2214/AJR.08.1694.
77. Maini R, Gadiraju TV, Jabbar A, Danrad R, Sweeney A. Cardiac MRI as a useful tool to differentiate tumor and thrombus. Int. J. Cardiovasc. Imaging. 2017;33:1795–6. https://doi.org/10.1007/s10554-017-1172-5.
78. Bittencourt MS, Achenbach S, Marwan M, Seltmann M, Muschiol G, Ropers D, et al. Left ventricular thrombus attenuation characterization in cardiac computed tomography angiography. J Cardiovasc Comput Tomogr. 2012;6:121–6. https://doi.org/10.1016/j.jcct.2011.12.006.
79. Paydarfar D, Krieger D, Dib N, Blair RH, Pastore JO, Stetz JJ, et al. In vivo magnetic resonance imaging and surgical histopathology of intracardiac masses: distinct features of subacute thrombi. Cardiology. 2001;95:40–7. https://doi.org/10.1159/000047342.
80. Kligerman S. Imaging of pericardial disease. Radiol Clin N Am. 2019;57:179–99. https://doi.org/10.1016/j.rcl.2018.09.001.
81. Fortuny E, Fernandez-Golfin C, Viliani D, Zamorano JL. Multimodality imaging in pericardial diseases. J Cardiovasc Echogr. 2012;22:1–10. https://doi.org/10.1016/j.jcecho.2011.09.004.
82. Fishman EK, Bluemke DA, Soyer P. Three-dimensional imaging: past, present and future. Diagn Interv Imaging. 2016;97:283–5. https://doi.org/10.1016/j.diii.2016.03.001.
83. Rowe SP, Johnson PT, Fishman EK. Initial experience with cinematic rendering for chest cardiovascular imaging. Br J Radiol. 2018. https://doi.org/10.1259/bjr.20170558.
84. Rowe SP, Johnson PT, Fishman EK. Cinematic rendering of cardiac CT volumetric data: principles and initial observations. J Cardiovasc Comput Tomogr. 2018;12:56–9. https://doi.org/10.1016/j.jcct.2017.11.013.
85. Dappa E, Higashigaito K, Fornaro J, Leschka S, Wildermuth S, Alkadhi H. Cinematic rendering – an alternative to volume rendering for 3D computed tomography imaging. Insights Imaging. 2016;7:849–56. https://doi.org/10.1007/s13244-016-0518-1.
86. Vukicevic M, Mosadegh B, Min JK, Little SH. Cardiac 3D printing and its future directions. JACC Cardiovasc Imaging. 2017;10:171–84. https://doi.org/10.1016/j.jcmg.2016.12.001.
87. Otton JM, Birbara NS, Hussain T, Greil G, Foley TA, Pather N. 3D printing from cardiovascular CT: a practical guide and review. Cardiovasc Diagn Ther. 2017;7:507–26. https://doi.org/10.21037/cdt.2017.01.12.
88. Yan C, Wang C, Pan X, Li S, Song H, Liu Q, Xu N, Wang J. Three dimensional printing assisted transcatheter closure of atrial septal defect with deficient posterior-inferior rim. Catheter Cardiovasc Interv. 2018 Dec 1;92(7):1309-1314.https://doi.org/10.1002/ccd.27799
89. Faganello G, Campana C, Belgrano M, Russo G, Pozzi M, Cioffi G, et al. Three dimensional printing of an atrial septal defect: is it multimodality imaging? Int. J. Cardiovasc. Imaging. 2016;32:427–8. https://doi.org/10.1007/s10554-015-0801-0.
90. Wang Z, Liu Y, Xu Y, Gao C, Chen Y, Luo H. Three-dimensional printing-guided percutaneous transcatheter closure of secundum atrial septal defect with rim deficiency: first-in-human series. Cardiol J. 2016;23:599–603. https://doi.org/10.5603/CJ.a2016.0094.
91. Chepelev L, Wake N, Ryan J, Althobaity W, Gupta A, Arribas E, et al. Radiological Society of North America (RSNA) 3D printing

Special Interest Group (SIG): guidelines for medical 3D printing and appropriateness for clinical scenarios. 3D Print Med. 2018;4:11. https://doi.org/10.1186/s41205-018-0030-y.

92. Schmauss D, Gerber N, Sodian R. Three-dimensional printing of models for surgical planning in patients with primary cardiac tumors. J Thorac Cardiovasc Surg. 2013;145:1407–8. https://doi.org/10.1016/j.jtcvs.2012.12.030.
93. Jacobs S, Grunert R, Mohr FW, Falk V. 3D-imaging of cardiac structures using 3D heart models for planning in heart surgery: a preliminary study. Interact Cardiovasc Thorac Surg. 2008;7:6–9. https://doi.org/10.1510/icvts.2007.156588.
94. Al Jabbari O, Abu Saleh WK, Patel AP, Igo SR, Reardon MJ. Use of three-dimensional models to assist in the resection of malignant cardiac tumors. J Card Surg. 2016;31:581–3. https://doi.org/10.1111/jocs.12812.
95. Valverde I, Gomez G, Suarez-Mejias C, Hosseinpour A-R, Hazekamp M, Roest A, et al. 3D printed cardiovascular models for surgical planning in complex congenital heart diseases. J Cardiovasc Magn Reson. 2015;17. https://doi.org/10.1186/1532-429x-17-s1-p196.